

Recombination and Annealing Pathways Compete for Substrates in Making *rrn* Duplications in *Salmonella enterica*

Andrew B. Reams,^{*†,1} Eric Kofoid,^{*} Natalie Duleba,^{*} and John R. Roth^{**}

^{*}Department of Microbiology and Molecular Genetics, University of California, Davis, California 95616, and [†]Department of Biological Sciences, California State University, Sacramento, California 95825

ABSTRACT Tandem genetic duplications arise frequently between the seven directly repeated 5.5-kb *rrn* loci that encode ribosomal RNAs in *Salmonella enterica*. The closest *rrn* genes, *rrnB* and *rrnE*, flank a 40-kb region that includes the *purHD* operon. Duplications of *purHD* arise by exchanges between *rrn* loci and form at a high rate (10^{-3} /cell/division) that remains high in strains blocked for early steps in recombination (*recA*, *recB*, and/or *recF*), but drops 30-fold in mutants blocked for later Holliday junction resolution (*rvuC* *recG*). The duplication defect of a *rvuC* *recG* mutant was fully corrected by an added mutation in any one of the *recA*, *recB*, or *recF* genes. To explain these results, we propose that early recombination defects activate an alternative single-strand annealing pathway for duplication formation. In wild-type cells, *rrn* duplications form primarily by the action of RecFORA on single-strand gaps. Double-strand breaks cannot initiate *rrn* duplications because *rrn* loci lack Chi sites, which are essential for recombination between two separated *rrn* sequences. A *recA* or *recF* mutation allows unrepaired gaps to accumulate such that different *rrn* loci can provide single-strand *rrn* sequences that lack the RecA coating that normally inhibits annealing. A *recB* mutation activates annealing by allowing double-strand ends within *rrn* to avoid digestion by RecBCD and provide a new source of *rrn* ends for use in annealing. The equivalent high rates of *rrn* duplication by recombination and annealing pathways may reflect a limiting economy of gaps and breaks arising in heavily transcribed, palindrome-rich *rrn* sequences.

THE most frequent tandem gene duplications in the *Salmonella* chromosome arise between directly repeated ribosomal RNA (*rrn*) loci (Anderson and Roth 1981; Reams *et al.* 2010). Duplications formed between such extensive repeats (5.5 kb) are generally thought to arise by unequal recombination between copies of the repeat in different sister chromosomes (Roth *et al.* 1996; Romero and Palacios 1997) (see Figure 1). Such exchanges are expected to depend heavily on the homologous recombination pathways that rely on the strand exchange enzyme RecA. In keeping with this expectation, duplications between chromosomal repeats of the *lac* operon form at high rates, comparable to those of *rrn* duplication, but depend heavily on RecA (A. Reams, M. Carter, and J. Roth unpublished results). In contrast, recent assays in two other situations suggest that RecA can be

dispensable for formation of duplications between long repeats that are subject to frequent nicks or breaks (Reams *et al.* 2010, 2012). Duplication of regions not flanked by extensive repeats are also RecA independent, but arise at rates two to three orders of magnitude lower than those for *rrn*-mediated duplications (Reams and Neidle 2003, 2004; Kugelberg *et al.* 2006; Reams *et al.* 2010). Here we describe duplications arising by exchanges between directly repeated *rrn* loci that are separated by >40 kb and are normal residents of the *Salmonella* chromosome. The goal is to understand how these duplications arise at such high rates with or without RecA.

Seven *rrn* loci are scattered around the *Salmonella enterica* chromosome (Figure 2) and have nearly identical base sequences. Recombination between these loci generates a variety of chromosome rearrangements including duplications, inversions, and translocations (Anderson and Roth 1981; Liu and Sanderson 1998; Helm *et al.* 2003). Tandem duplications between *rrn* loci form at very high rates. For example, the *argH* gene, between *rrnA* and *rrnB* (see Figure 2), duplicates at 1.9×10^{-3} /cell/division (Reams *et al.* 2010), and this rate is essentially unaltered in *recA* mutants (Reams

Copyright © 2014 by the Genetics Society of America
doi: 10.1534/genetics.113.158519

Manuscript received August 23, 2013; accepted for publication October 17, 2013;
published Early Online November 1, 2013.

¹Corresponding author: Department of Biological Sciences, California State University, 6000 J Street, Sacramento, CA 95819-6077 E-mail: andrew.reams@csus.edu

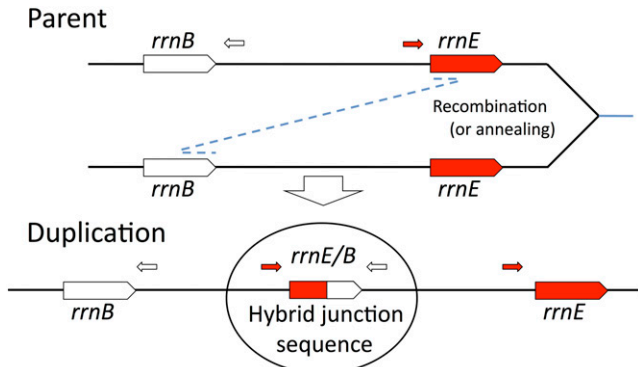


Figure 1 Process of duplication formation and join-point identification. The duplications described here arise by genetic exchanges between different *rrn* loci in sister chromosomes and may occur by recombination or by single-strand annealing. Duplications were trapped, and their *rrn* junction sequences were amplified using PCR with primers that diverge in the parent sequence but converge at a duplication junction (circled). Only the *rrnE/B* duplication is diagrammed here. The diagram and the text discuss the critical exchange required for duplication without regard to reciprocity or to the ultimate fate of unjoined ends.

et al. 2010). These duplications of *argH* are lost at a 10-fold higher rate (10^{-2} /cell/division) by heavily RecA-dependent recombination between the extensive duplicated regions (>150 kb). Because of their high loss rate and fitness cost, *argH* duplications are carried as stable polymorphisms in unselected cultures and are maintained at a steady-state frequency of $\sim 1\%$ (Reams *et al.* 2010). These high steady-state frequencies are likely to be a general property of all duplications in all organisms.

The surprising RecA independence of *rrn*-mediated duplication formation is examined here using the *purHD* locus. This region is flanked by the most closely spaced *rrn* cistrons, *rrnB* and *rrnE* (separated by 40 kb), and is held at the highest duplication steady-state frequency ($\sim 3\%$) of any tested point in the chromosome (Anderson and Roth 1981). It is suggested that the high rate and apparent recombination independence of *rrn* duplications may reflect two features of *rrn* sequences. First, *rrn* cistrons are the most highly transcribed genes in the *Salmonella* and *Escherichia coli* chromosomes (Dennis 2004). Second, *rrn* sequences include many stem-loop structures that are responsible for folding of the ribosomal RNAs (16S, 23S, 5S) produced from each locus. The palindromic features of *rrn* DNA may allow untranscribed strands to form secondary structures that are subject to cutting or breakage. These unusual features may make *rrn* sequences prone to frequent gaps and breaks.

It is proposed here that blockage of early recombination steps (RecBCDA and RecFORA) can activate a single-strand annealing pathway of duplication formation that compensates for loss of recombination. When frequent DNA damage within *rrn* sequences remains unrepaired by recombination, these lesions can accumulate sufficiently that two different *rrn* loci can provide ends. Duplications can form by annealing when two single-strand ends are provided and neither strand is coated with inhibitory RecA protein. Activation of

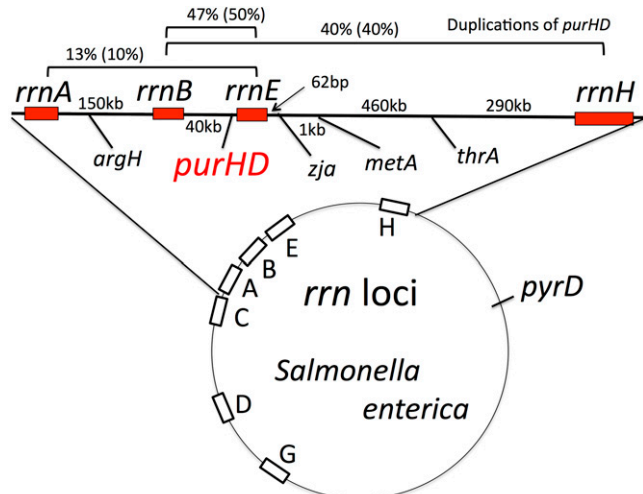


Figure 2 Positions of *rrn* loci and nature of *purHD* duplication endpoints. The genetic map indicates the position of *rrn* loci on the circular *S. enterica* chromosome. The expanded top region shows the *purHD* region analyzed here. Map distances are not to scale. The distribution of duplications that include the *purHD* locus is based on 30 *purH* duplications isolated in a *recA*⁺ strain and 20 duplications (in parentheses) isolated in a *recA* mutant strain.

annealing pathways renders duplication formation independent of Holliday resolution activities (RuvC, RecG).

Materials and Methods

Strains and media

All strains were derivatives of *S. enterica* (Typhimurium) strain LT2 and are listed in Table 1. Rich medium was Luria broth (LB), used with antibiotics as described below.

Trapping duplications formed in overnight cultures

The drug-in-drug method for measuring duplication frequencies in unselected overnight cultures was described previously (Reams *et al.* 2010, 2012). For these assays, the strain to be tested carries the *tetAR* genes for tetracycline resistance (Tc^R) inserted as part of transposon Tn10 into the test locus (e.g., *purH*). These strains are then made sensitive to tetracycline by a kanamycin-resistance (Kn^R) determinant inserted into the *tetA* gene. The resulting strains are phenotypically Tc^S Kn^R. Duplications are trapped by a Red-mediated recombineering cross in which a short single-strand fragment (80 bases) is introduced into the tested strain, which carries a pSIM5 plasmid and is grown at 30° (Court *et al.* 2002). This fragment, introduced at 42°, restores Tc^R by precisely excising the Kn^R determinant. Transformants are selected on LB-tetracycline agar plates. The majority of these transformants become Tet^R Kan^S. However, any recipient cells with a pre-existing duplication of the test locus become Tet^R, but retain their Kan^R phenotype and are detected by replica-printing to LB-tetracycline-kanamycin. Duplication frequencies are calculated by dividing the number of Tc^R Kn^R colonies by the total number of Tc^R colonies. Duplication of *purHD* by exchanges

Table 1 Strains used in this study

Strain	Genotype ¹	Source
TR10000	Wild-type <i>S. enterica</i> (serovar Typhimurium) LT2	Lab collection
TT25620	<i>purH887::Tn10, tetA101::Kan(Tc^SKn^R)</i> DEL(Fels-2 Gifsy-1 Gifsy-2) <i>sulA46::Spc lexA34::Rif(sw)/pSIM5(Cm^R)</i>	This report
TT25621	<i>purH887::Tn10, tetA101::Kan(Tc^SKn^R)</i> DEL(Fels-2 Gifsy-1 Gifsy-2) <i>sulA46::Spc lexA34::Rif(sw) recA650::Gnt(sw)/pSIM5(Cm^R)</i>	This report
TT25671	<i>purH887::Tn10, tetA101::Kan(Tc^SKn^R)</i> DEL(Fels-2 Gifsy-1 Gifsy-2) <i>sulA46::Spc lexA33:(Rif lexA3IND)/pSIM5(Cm^R)</i>	This report
TT25672	<i>purH887::Tn10, tetA101::Kan(Tc^SKn^R)</i> DEL(Fels-2 Gifsy-1 Gifsy-2) <i>sulA46::Spc lexA33:(Rif lexA3IND) recA650::Gnt(sw)/pSIM5(Cm^R)</i>	This report
TT26376	<i>zja9229::tetRA(sw); tetA101::Kan (Tc^SKn^R)/pSIM5(Cm^R)</i>	This report
TT26377	<i>metA2382::tetRA(sw); tetA101::Kan (Tc^SKn^R)/pSIM5(Cm^R)</i>	This report
TT26379	<i>thrA537::tetRA(sw); tetA101::Kan (Tc^SKn^R)/pSIM5(Cm^R)</i>	This report
TT26380	<i>zja9229::tetRA(sw); tetA101::Kan (Tc^SKn^R) rrnE::GntR(sw)/pSIM5(Cm^R)</i>	This report
TT26381	<i>metA2382::tetRA(sw); tetA101::Kan (Tc^SKn^R) rrnE::GntR(sw)/pSIM5(Cm^R)</i>	This report
TT26382	<i>thrA537::tetRA(sw); tetA101::Kan (Tc^SKn^R) rrnE::GntR (sw)/pSIM5(Cm^R)</i>	This report
TT26402	<i>thrA537::tetRA(sw); tetA101::Kan (Tc^SKn^R) rrnH::Spc (sw)/pSIM5(Cm^R)</i>	This report
TT26403	<i>thrA537::tetRA(sw); tetA101::Kan (Tc^SKn^R) rrnH::Spc(sw) rrnE::GntR(sw)/pSIM5(Cm^R)</i>	This report
TT26404	<i>metA2382::tetRA(sw); tetA101::Kan (Tc^SKn^R) rrnH::Spc(sw)/pSIM5(Cm^R)</i>	This report
TT26405	<i>metA2382::tetRA(sw); tetA101::Kan (Tc^SKn^R) rrnE::Gnt(sw) rrnH::Spc(sw)/pSIM5(Cm^R)</i>	This report
TT26406	<i>zja9229::tetRA(sw); tetA101::Kan (Tc^SKn^R) rrnH::Spc(sw)/pSIM5(Cm^R)</i>	This report
TT26407	<i>zja9229::tetRA(sw); tetA101::Kan (Tc^SKn^R) rrnE::Gnt(sw) rrnH::Spc(sw)/pSIM5(Cm^R)</i>	This report
TT26438	<i>purH2411::tetAR; tetA101::Kan(Tc^SKn^R)/pSIM5(Cm^R)</i>	This report
TT26439	<i>purD2412::tetAR; tetA101::Kan(Tc^SKn^R)/pSIM5(Cm^R)</i>	This report
TT26441	<i>purD2412::tetAR; tetA101::Kan(Tc^SKn^R) recF521::Tn5d-Rif/pSIM5(Cm^R)</i>	This report
TT26442	<i>purH2411::tetAR; tetA101::Kan(Tc^SKn^R) recF521::Tn5d-Rif/pSIM5(Cm^R)</i>	This report
TT26443	<i>purD2412::tetAR; tetA101::Kan(kanR) ruvC4::Rif(sw)/pSIM5(Cm^R)</i>	This report
TT26444	<i>purH2411::tetAR; tetA101::Kan(Tc^SKn^R) ruvC4::Rif(sw)/pSIM5(Cm^R)</i>	This report
TT26445	<i>purD2412::tetAR; tetA101::Kan(Tc^SKn^R) recA650::Gnt(sw)/pSIM5(Cm^R)</i>	This report
TT26446	<i>purD2412::tetAR; tetA101::Kan(Tc^SKn^R) recA651::Rif(sw)/pSIM5(Cm^R)</i>	This report
TT26461	<i>purH2411::tetAR; tetA101::Kan(Tc^SKn^R) recA650::Gnt(sw)/pSIM5(Cm^R)</i>	This report
TT26462	<i>purH2411::tetAR; tetA101::Kan(Tc^SKn^R) recA651::Rif(sw)/pSIM5(Cm^R)</i>	This report
TT26463	<i>purH2411::tetAR; tetA101::Kan(Tc^SKn^R) recB10 his646(del:OGD) pro-47(del:AB)/pSIM5(Cm^R)</i>	This report
TT26464	<i>purD2412::tetAR; tetA101::Kan(Tc^SKn^R) recB10 his646(del:OGD) pro-47(del:AB)/pSIM5(Cm^R)</i>	This report
TT26465	<i>purH2411::tetAR; tetA101::Kan(Tc^SKn^R) DEL1742(argA-recB)/pSIM5(Cm^R)</i>	This report
TT26466	<i>purD2412::tetAR; tetA101::Kan(Tc^SKn^R) DEL1742(argA-recB)/pSIM5(Cm^R)</i>	This report
TT26467	<i>purH2411::tetAR; tetA101::Kan(Tc^SKn^R) recF521::Tn5d-Rif recB10 his646(del:OGD) pro-47(del:AB)/pSIM5(Cm^R)</i>	This report
TT26468	<i>purD2412::tetAR; tetA101::Kan(Tc^SKn^R) recF521::Tn5d-Rif recB10 his646(del:OGD) pro-47(del:AB)/pSIM5(Cm^R)</i>	This report
TT26469	<i>purH2411::tetAR; tetA101::Kan(Tc^SKn^R) recF521::Tn5d-Rif DEL1742(argA-recB)/pSIM5(Cm^R)</i>	This report
TT26470	<i>purD2412::tetAR; tetA101::Kan(Tc^SKn^R) recF521::Tn5d-Rif DEL1742(argA-recB)/pSIM5(Cm^R)</i>	This report
TT26498	<i>purH2411::tetAR; tetA101::Kan(Tc^SKn^R) ruvAB7::Spc(sw)/pSIM5(Cm^R)</i>	This report
TT26500	<i>purH2411::tetAR; tetA101::Kan(Tc^SKn^R) recN655::Spc(sw)/pSIM5(Cm^R)</i>	This report
TT26502	<i>purD2412::tetAR; tetA101::Kan(Tc^SKn^R) recN655::Spc(sw)/pSIM5(Cm^R)</i>	This report
TT26507	<i>purH2411::tetAR; tetA101::Kan(Tc^SKn^R) recG646::Rif(sw) ruvC4::Spc(sw)/pSIM5(Cm^R)</i>	This report
TT26508	<i>purD2412::tetAR; tetA101::Kan(Tc^SKn^R) recG646::Rif(sw) ruvC4::Spc(sw)/pSIM5(Cm^R)</i>	This report
TT26522	<i>purH2411::tetAR; tetA101::Kan(Tc^SKn^R) ruvAB7::Spc(sw) recA650::Gnt(sw)/pSIM5(Cm^R)</i>	This report
TT26528	<i>purD2412::tetAR; tetA101::Kan(kanR) ruvAB7::Spc(sw)/pSIM5(Cm^R)</i>	This report
TT26530	<i>purD2412::tetAR; tetA101::Kan(kanR) ruvAB7::Spc(sw) recA650::Gnt(sw)/pSIM5(Cm^R)</i>	This report
TT26532	<i>purD2412::tetAR; tetA101::Kan(Tc^SKn^R) DELmutS281/pSIM5(Cm^R)</i>	This report
TT26534	<i>purD2412::tetAR; tetA101::Kan(kanR) ruvC4::Rif(sw) recA650::Gnt(sw)/pSIM5(Cm^R)</i>	This report
TT26536	<i>purH2411::tetAR; tetA101::Kan(Tc^SKn^R) ruvC4::Rif(sw) recA650::Gnt(sw)/pSIM5(Cm^R)</i>	This report
TT26537	<i>purH2411::tetAR; tetA101::Kan(Tc^SKn^R) recG646::Rif(sw)/pSIM5(Cm^R)</i>	This report
TT26538	<i>purD2412::tetAR; tetA101::Kan(Tc^SKn^R) recG646::Rif(sw)/pSIM5(Cm^R)</i>	This report
TT26540	<i>purH2411::tetAR; tetA101::Kan(Tc^SKn^R) recG646::Rif(sw) ruvC4::Spc(sw) recA650::Gnt(sw)/pSIM5(Cm^R)</i>	This report
TT26542	<i>purD2412::tetAR; tetA101::Kan(Tc^SKn^R) recG646::Rif(sw) ruvC4::Spc(sw) recA650::Gnt(sw)/pSIM5(Cm^R)</i>	This report
TT26545	<i>purH2411::tetAR; tetA101::Kan(Tc^SKn^R) recG646::Rif(sw) recA650::Gnt(sw)/pSIM5(Cm^R)</i>	This report
TT26546	<i>purD2412::tetAR; tetA101::Kan(Tc^SKn^R) recG646::Rif(sw) recA650::Gnt(sw)/pSIM5(Cm^R)</i>	This report
TT26477	<i>pyrD2828::tetAR; tetA101::Kan(Tc^SKn^R)/pSIM5(Cm^R)</i>	This report
TT26479	<i>pyrD2828::tetAR; tetA101::Kan(Tc^SKn^R) recA651::Rif(sw)/pSIM5(Cm^R)</i>	This report
TT26551	<i>purH2411::tetAR; tetA101::Kan(Tc^SKn^R) rrnE::GntR(sw)/pSIM5(Cm^R)</i>	This report
TT26552	<i>purH2411::tetAR; tetA101::Kan(Tc^SKn^R) rrnE::GntR(sw) rrnH::Spc(sw)/pSIM5(Cm^R)</i>	This report
TT26553	<i>purD2412::tetAR; tetA101::Kan(Tc^SKn^R) rrnE::GntR(sw) rrnH::Spc(sw)/pSIM5(Cm^R)</i>	This report
TT26556	<i>purH2411::tetAR; tetA101::Kan(Tc^SKn^R) recN655::Spc(sw) recA650::Gnt(sw)/pSIM5(Cm^R)</i>	This report

(continued)

Table 1, continued

Strain	Genotype ¹	Source
TT26557	<i>purD2412::tetAR; tetA101::Kan(Tc^SKn^R) recN655::Spc(sw) recA650::Gnt(sw)/pSIM5(Cm^R)</i>	This report
TT26559	<i>purH2411::tetAR; tetA101::Kan(Tc^SKn^R) rrmH::Spc(sw)/pSIM5(Cm^R)</i>	This report
TT26563	<i>purD2412::tetAR; tetA101::Kan(Tc^SKn^R) rrmH::Spc(sw)/pSIM5(Cm^R)</i>	This report
TT26567	<i>purH2411::tetAR; tetA101::Kan(Tc^SKn^R) DEL1742(argA-recB) recA650::Gnt(sw)/pSIM5(Cm^R)</i>	This report
TT26569	<i>purD2412::tetAR; tetA101::Kan(Tc^SKn^R) DEL1742(argA-recB) recA650::Gnt(sw)/pSIM5(Cm^R)</i>	This report
TT26571	<i>purH2411::tetAR; tetA101::Kan(Tc^SKn^R) recF521::Tn5d-Rif DEL1742(argA-recB) recA650::Gnt(sw)/pSIM5(Cm^R)</i>	This report
TT26573	<i>purD2412::tetAR; tetA101::Kan(Tc^SKn^R) recF521::Tn5d-Rif DEL1742(argA-recB) recA650::Gnt(sw)/pSIM5(Cm^R)</i>	This report
TT26578	<i>purD2412::tetAR; tetA101::Kan(Tc^SKn^R) DEL(Fels-2) leuA414(UAG) sbcB1 recA651::Rif(sw)/pSIM5(Cm^R)</i>	This report
TT26581	<i>purD2412::tetAR; tetA101::Kan(Tc^SKn^R) sbcB::Zeo(sw)/pSIM5(Cm^R)</i>	This report
TT26584	<i>purH2411::tetAR; tetA101::Kan(Tc^SKn^R) sbcCD::Gnt(sw) recA651::Rif(sw)/pSIM5(Cm^R)</i>	This report
TT26587	<i>purD2412::tetAR; tetA101::Kan(Tc^SKn^R) sbcCD::Gnt(sw) recA651::Rif(sw)/pSIM5(Cm^R)</i>	This report
TT26589	<i>purH2411::tetAR; tetA101::Kan(Tc^SKn^R) recO656::GntR(sw)/pSIM5(Cm^R)</i>	This report
TT26591	<i>purH2411::tetAR; tetA101::Kan(Tc^SKn^R) recO656::GntR(sw) recA651::Rif(sw)/pSIM5(Cm^R)</i>	This report
TT26593	<i>purD2412::tetAR; tetA101::Kan(Tc^SKn^R) recO656::GntR(sw)/pSIM5(Cm^R)</i>	This report
TT26595	<i>purD2412::tetAR; tetA101::Kan(Tc^SKn^R) recO656::GntR(sw) recA651::Rif(sw)/pSIM5(Cm^R)</i>	This report
TT26596	<i>purH2411::tetAR; tetA101::Kan(Tc^SKn^R) sbcCD::Gnt(sw)/pSIM5(Cm^R)</i>	This report
TT26597	<i>purD2412::tetAR; tetA101::Kan(Tc^SKn^R) rrmE::GntR(sw)/pSIM5(Cm^R)</i>	This report
TT26603	<i>purH2411::tetAR; tetA101::Kan(Tc^SKn^R) recQ::Spc(sw) recA651::Rif(sw)/pSIM5(Cm^R)</i>	This report
TT26605	<i>pyrD2828::tetAR; tetA101::Kan(Tc^SKn^R) recG646::Rif(sw) ruvC6::Spc(sw)/pSIM5(Cm^R)</i>	This report
TT26607	<i>purD2412::tetAR; tetA101::Kan(Tc^SKn^R) recG646::Rif(sw) ruvC4::Spc(sw) recF521::Tn5d-Rif DEL1742(argA-recB)/pSIM5(Cm^R)</i>	This report
TT26613	<i>purD2412::tetAR; tetA101::Kan(Tc^SKn^R) recF521::Tn5d-Rif recA650::Gnt(sw)/pSIM5(Cm^R)</i>	This report
TT26615	<i>purH2411::tetAR; tetA101::Kan(Tc^SKn^R) recF521::Tn5d-Rif recA650::Gnt(sw)/pSIM5(Cm^R)</i>	This report
TT26618	<i>purD2412::tetAR; tetA101::Kan(Tc^SKn^R) DEL(Fels-2) leuA414(UAG) sbcB1/pSIM5(Cm^R)</i>	This report
TT26622	<i>purH2411::tetAR; tetA101::Kan(Tc^SKn^R) recG646::Rif(sw) ruvC4::Spc(sw) DEL1742(argA-recB)/pSIM5(Cm^R)</i>	This report
TT26625	<i>purD2412::tetAR; tetA101::Kan(Tc^SKn^R) recG646::Rif(sw) ruvC4::Spc(sw) DEL1742(argA-recB)/pSIM5(Cm^R)</i>	This report
TT26628	<i>purH2411::tetAR; tetA101::Kan(Tc^SKn^R) recG646::Rif(sw) ruvC4::Spc(sw) recF521::Tn5d-Rif DEL1742(argA-recB)/pSIM5(Cm^R)</i>	This report
TT26632	<i>purH2411::tetAR; tetA101::Kan(Tc^SKn^R) recJ657::Rif(sw)/pSIM5(Cm^R)</i>	This report
TT26634	<i>purH2411::tetAR; tetA101::Kan(Tc^SKn^R) recJ657::Rif(sw) recA650::Gnt(sw)/pSIM5(Cm^R)</i>	This report
TT26636	<i>purD2412::tetAR; tetA101::Kan(Tc^SKn^R) recJ657::Rif(sw)/pSIM5(Cm^R)</i>	This report
TT26638	<i>purD2412::tetAR; tetA101::Kan(Tc^SKn^R) recJ657::Rif(sw) recA650::Gnt(sw)/pSIM5(Cm^R)</i>	This report
TT26640	<i>purH2411::tetAR; tetA101::Kan(Tc^SKn^R) ligB::Rif(sw)/pSIM5(Cm^R)</i>	This report
TT26642	<i>purH2411::tetAR; tetA101::Kan(Tc^SKn^R) ligB::Rif(sw) recA650::Gnt(sw)/pSIM5(Cm^R)</i>	This report
TT26644	<i>purD2412::tetAR; tetA101::Kan(Tc^SKn^R) ligB::Rif(sw)/pSIM5(Cm^R)</i>	This report
TT26646	<i>purD2412::tetAR; tetA101::Kan(Tc^SKn^R) ligB::Rif(sw) recA650::Gnt(sw)/pSIM5(Cm^R)</i>	This report
TT26657	<i>purD2412::tetAR; tetA101::Kan(Tc^SKn^R) recG646::Rif(sw) ruvC4::Spc(sw) recF521::Tn5d-Rif/pSIM5(Cm^R)</i>	This report
TT26660	<i>purH2411::tetAR; tetA101::Kan(Tc^SKn^R) recG646::Rif(sw) ruvC4::Spc(sw) recF521::Tn5d-Rif/pSIM5(Cm^R)</i>	This report
TT26806	<i>purD2412::tetAR; tetA101::Kan(Tc^SKn^R) DELmutS281 recA650::Gnt(sw)/pSIM5(Cm^R)</i>	This report
TT26833	<i>pyrD2828::tetAR; tetA101::Kan(Tc^SKn^R) ruvC6::Spc(sw) recG646::Rif(sw) recA650::Gnt(sw)/pSIM5(Cm^R)</i>	This report

"sw" designates alleles in which the normal sequence was replaced by a drug resistance determinant. "tetA101::Kan (Tc^SKn^R)" refers to a kanamycin resistance determinant inserted into the middle of the *tetA* gene, rendering the strain sensitive to tetracycline and resistant to kanamycin. The "pSIM5(Cm^R)" plasmid carries the recombination genes (red) of phage lambda (Court *et al.* 2002).

between *rrn* loci was verified by join-point PCR and whole-genome sequencing (see below).

The rate of duplication formation is defined here as "the duplication frequency attained by a culture during 33 generations of growth from a single cell without a duplication." This frequency is below the steady-state level, and the nearly linear accumulation of duplications in this period is taken as the initial rate of duplication formation. The course of duplication accumulation was described previously (Reams *et al.* 2010). The forces that drive duplication frequency toward a steady state minimize the effects of Luria-Delbrück fluctuation. Low viability of some *rec* mutant strains does not interfere with comparison of rates to those in wild type because each rate is based on the fraction of viable tester cells that carry a duplication. The 33-generation period is assured by a single colony isolating the strain to be

assayed and using an entire small colony to inoculate a liquid culture (4 ml) that is grown to stationary phase. The final titer (2×10^9 cells) is achieved after 33 generations of growth of the cell that initiated the colony.

Duplication join-point analysis

Trapped *purHD* duplications were analyzed for the nature of their *rrn*-mediated join points using a divergent primer PCR method described previously (Helm and Maloy 2001). Two divergent primers direct synthesis in opposite directions away from *purHD*. The primers anneal to regions immediately adjacent to various *rrn* locus (Figure 2). Since these primers direct divergent replication, a PCR product will be amplified only in strains with a specific *rrn*-mediated duplication junction. The following primer pairs were used to test for the presence of the various hybrid *rrn* combinations

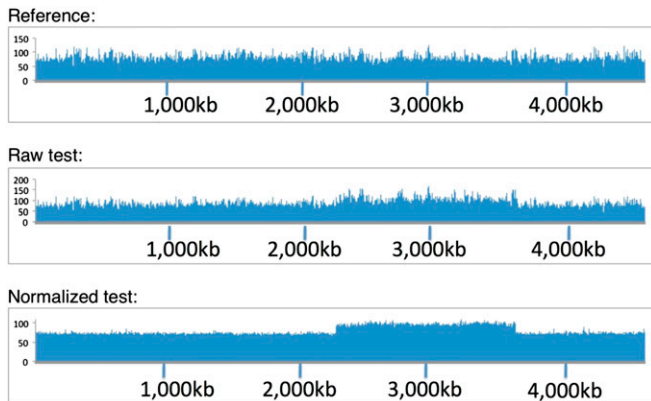


Figure 3 Identification of duplications by read-depth profiles. Full-genome sequences were determined (Illumina) for a haploid parent reference strain (top) and strain in which about half of the cells carried a duplication (middle). The duplication was clearer when the read-depth profile of the experimental strain was normalized to that of the parent (bottom).

possible for *purHD* duplications: *rrnE/B* (TP2306+TP2311), *rrnH/B* (TP2306+TP2315), *rrnE/H* (TP2311+TP2316), *rrnE/A* (TP2304+TP2311), *rrnH/A* (TP2304+TP2315), *rrnE/C* (TP2308+TP2311), *rrnH/C* (TP2308+TP2315). The sequences of these primers are TP2304 (5' TGCCTTCATAAGCGGTGGTTAGAG 3'), TP2306 (5' CCAGGCGCTCAGTAGTTGTTGTTCG 3'), TP2308 (5' GCTGTTAGGGCACTTCACCTTGCGC 3'), TP2311 (5' CGATAGGGCGATGTGGTGCTGTTC 3'), TP2315 (5' CCATCCGCAGGGCAGCATAGAAGAG 3'), and TP2316 (5' CGGCAATAGCCTTTCCATCAACGG 3').

Prior to PCR, both the parent and various trapped *purHD* duplication strains were grown overnight in 2 ml LB media and diluted 10-fold. For each divergent primer pair, a PCR reaction was run on each strain. All PCR products were separated on a 0.7% agarose gel using standard electrophoresis procedures and visualized after staining with ethidium bromide. Strains carrying a duplication specific to the applied primers generated an ~7-kb PCR product, whereas the parent strains showed no PCR product. Using this method, the specific *rrn* locus involved in forming the duplication was determined for all 30 of the tested *purHD* duplications. Whole-genome sequencing of several strains verified their PCR-determined *rrn* join points and demonstrated the presence of a simple duplication.

The crossover points of the exchanges that generated the hybrid *rrn* duplication join points were determined by sequencing the gel-purified 7-kb PCR products derived from junctions of independently isolated *purHD* duplications. PCR products were sequenced using 12 different primers that covered the entire *rrn* region. The sequences of hybrid junction elements were compared to those of participating parent *rrn* loci. The crossover event was inferred to have occurred in the region where the hybrid *rrn* sequence of one *rrn* sequence (e.g., *rrnE*) transitioned to that of another (e.g., *rrnE*).

Normalization of read-depth plots

Plots of Illumina read-depth data are often noisy due to uneven amplification in the PCR step of library preparation and from the

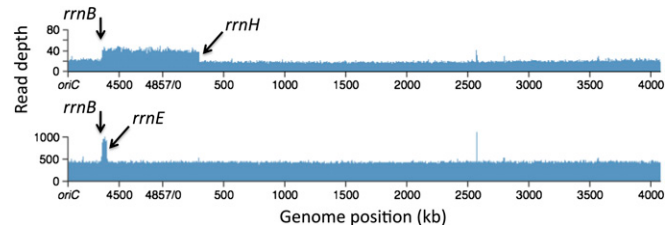


Figure 4 Genomic read-depth profile of a duplication strain. The read depth of a whole-genome sequence of a duplication strain (Illumina) was normalized to that of the parent strain. (Top) Results for a strain shown by PCR to have a *rrnE/B* junction, and (Bottom) A strain with an *rrnH-rrnB* junction. The few narrow spikes (bp 2500–3000) are not present in the raw data and are generated by the normalization process due to small deletion mutations carried by the standard strain.

effects of G+C differences on detection chemistry and DNA fragmentation. Since the profile is remarkably uniform between isogenic strains, the noise can be filtered out by comparing data from an isogenic reference strain (preferably from the same run). A normalization factor is determined at each position and used to correct the depth of the test genome, yielding a graph that clarifies the features of interest. An example is shown in Figure 3. The duplication strain tested was a population in which half the cells contained a large duplication. The duplication was unrecognized initially, but became clear following normalization.

Results

Duplications of the *purHD* operon arise between flanking *rrn* genes

Duplications were trapped as described previously (Reams *et al.* 2010), and junction points were classified by using PCR to determine which *rrn* loci recombined to form the duplication. For example, in identifying the *rrnE/B* junction (see Figure 1), one primer was directed clockwise toward *rrnE* and the other was directed counterclockwise toward *rrnB* as described previously (Helm and Maloy 2001). Cultures were diluted before DNA preparation to assure that the dominant structure was assayed and minimize contributions from any new *rrn* duplications appearing during growth. The presence of a *rrnE/B* duplication junction was demonstrated by production of a 7-kb PCR product using divergent primers (*rrnE* and *rrnB*). Other divergent primer pairs tested the presence of the various *rrn* join-point combinations studied here (e.g., *rrnH/B*, *rrnA/E*).

As seen in Figure 2, all 30 *purHD* duplications trapped in a *recA*⁺ strain showed hybrid *rrn* join points. Most (47%) involved the smallest interval (*rrnE/B*). Next most frequent (40%) were *rrnH/B*, and 13% involved *rrnA/E* (see Figure 2). None of the other *rrn* pairs flanking *purHD* were detected (*rrnH/C*, *rrnH/A*, *rrnE/C*). Several of the characterized *rrn*-mediated duplications were further analyzed by whole-genome sequencing. As seen in Figure 4, the Illumina read depth is elevated twofold for the genomic region between the corresponding *rrn* loci. This confirms that the

trapped duplications carry two copies of the intervening region corresponding to the join point determined by PCR and no other obvious rearrangements.

Dependence of duplication rates on flanking *rrn* sequences

The duplication rate of the *purHD* operon is defined here as the duplication frequency attained during 33 generations of growth from a single cell lacking a duplication. During this period the frequency of *purHD* duplications reached 2.5%, a rate that corresponds to 3×10^{-3} /cell/generation. This increase is nearly linear and is taken as an initial rate since it is far from the ultimate steady-state frequency.

The duplication rates of *purHD* and three nearby loci (*zja*, *metA*, and *thrA*) were assayed in strains lacking either or both of the *rrnE* and *rrnH* sequences. Positions of these loci are shown in Figure 2. Removal of both *rrnE* and *rrnH* caused a large decrease (170-fold) in the *purHD* duplication rate (Table 2). The duplication rates for the *zja*, *metA*, and *thrA* sites showed a similar drop after deletion of only *rrnH*. In all cases, the large drop in duplication rate resulted from removal of all the *rrn* loci from one side of the test site. The few residual duplications seen in these *rrn*-deficient backgrounds arose between diverse short sequence repeats and will be described elsewhere (A. Reams, E. Kofoid, and J. Roth, unpublished results).

As seen in Figure 2, roughly half of the *purHD* duplications arose by exchanges between *rrnB* and *rrnE*. Nevertheless, removal of *rrnE* alone had very little effect on the *purHD* duplication rate (Table 2), while removal of *rrnH* alone caused a fivefold reduction. The relatively large contribution of *rrnH* to the *purHD* duplication rate is not understood. We suggest that *rrnH* may be subject to more frequent chromosome gaps or breaks than *rrnE*, making *rrnH/B* duplications form more frequently than *rrnE/B* types. However, the larger (790 kb) *rrnH/B* duplication may have a higher fitness cost, leading to selective deletion of the region between *rrnE* and *rrnH* either before or after being trapped. Such remodeling would maintain the duplication state of *purHD*, but would leave a shorter (40 kb), lower-cost duplication with a *rrnE/B* join point.

Three sites in the chromosomal region between *rrnE* and *rrnH* (*zja*, *metA*, and *thrA*) were found to be duplicated at a slightly lower rate than *purHD* (see Table 2). Removal of *rrnE* had very little effect on the duplication rate of these loci, suggesting that most of these duplications form between *rrnB* and *rrnH*. The few duplications of this region that formed in strains without *rrnH* (for which *rrn*-mediated duplications are impossible) showed join points, suggesting that they arose by exchanges between diverse short sequences (A. Reams, E. Kofoid, and J. Roth, unpublished results).

Duplication rates are unaffected by defects in early steps of homologous recombination

The large size of the flanking *rrn* repeats and the high frequency of exchanges between them suggested that duplications of *purHD* are likely to form by homologous recombination. Strong RecA dependence has been seen in many situations in

Table 2 Effect of *rrn* deletions on rates of duplication formation

Deleted <i>rrn</i> loci	Duplication rate ^a of indicated sites with or without deletions of <i>rrn</i> loci ($\times 100$)			
	<i>purHD</i>	<i>zja</i>	<i>metA</i>	<i>thrA</i>
None	250	200	220	160
<i>rrnE</i>	210	100	200	100
<i>rrnH</i>	50	1.1	2.7	0.5
<i>rrnE</i> and <i>rrnH</i>	1.5	0.7	2.5	0.8

^a Duplication rates are expressed as the frequency of duplication-bearing cells reached during growth of a cell with no duplication for 33 generations.

which duplications form between extensive perfect repeats (Roth *et al.* 1996; Romero and Palacios 1997). However, *purHD* duplication rates are essentially unaffected by mutations that eliminate enzymes important to standard pathways of recombination (see Figure 5). Furthermore, the distribution of junction types (*rrnE/B*, *rrnH/B*, and *rrnE/A*) for *purHD* duplications were the same in *recA*⁺ and *recA* mutant strains (see Figure 2, top). Taken at face value, these results suggest that RecA, RecB, or RecF enzymes are not involved in duplication formation. Despite these phenotypes, we suggest below that formation of these duplications in wild-type strains is heavily recombination dependent and occurs by single-strand annealing only in strains lacking these recombination functions.

The apparent RecA independence of *rrn* duplications suggested formation by single-strand annealing. Alternatively, RecA-independent events might be illegitimate exchanges mediated by topoisomerases that are likely to act within or near *rrn* loci in response to heavy transcription of these loci. The exchanges that produce duplications are not associated with formation of deletions or duplications within the *rrn* locus since the size of the *rrn* locus at the join point is as expected for a simple hybrid recombinant. To learn more about the nature of the exchanges, we analyzed hybrid *rrn* junction sequences to determine the approximate points within the *rrn* loci at which the genetic exchanges occurred. This is possible because the base sequences of different *rrn* loci are not identical. Each locus has sequence features that are unique, and every pair of *rrn* loci differs at several points. A tree of *rrn* sequence difference in the Appendix describes their differences. The aligned sequences of the three *rrn* loci involved in duplicating the *purHD* operon are diagrammed in Figure 6, where regions with many clustered sequence differences are boxed, and isolated single-base differences are indicated by colored triangles.

To determine the location of the crossover point that formed the duplication, the hybrid junction *rrn* loci were amplified from independently isolated duplications and their sequences were compared to those of the two parental *rrn* sequences. Figure 6 describes the exchange points of 26 independent *rrnE/B* duplications and 7 *rrnH/B* duplications isolated from *recA*⁺ and *recA* mutant strains. For each duplication, the exchange fell within one of three regions of extended sequence identity. Most crossover events occurred within region III, the largest window of perfect identity (2390 bp for

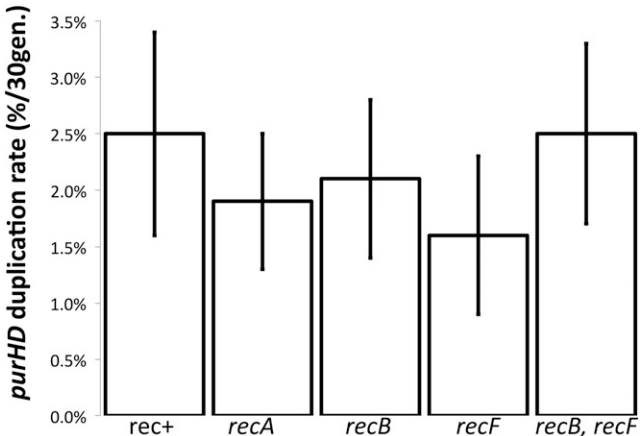


Figure 5 Duplication rates in several mutants defective for homologous recombination. Duplication rates were measured by determining the frequency of *purHD* duplication after 33 generations of growth from a single cell lacking a duplication. The frequency of duplications attained within this period is taken as the initial rate of duplication formation. The rates presented here are based on combined data for *purD* and the adjacent *purH* gene. Both sites individually gave essentially the same result.

rrnE/B or 2490 bp for *rrnH/B*), while fewer events occurred within the other two smaller windows, region I (756 bp for *rrnE/B* and *rrnH/B*) or region II (497 bp for *rrnE/B* and 413 bp for *rrnH/B*). Duplications trapped in *rec⁺* and *recA* backgrounds showed a similar distribution of exchange points.

The results in Figure 6 suggest either that *rrn*-mediated duplications form by the same pathway in *rec⁺* and *recA* strains or that homologous recombination and single-strand annealing pathways lead to the same distribution of exchange points. The results do not exclude the possibility that topoisomerase catalyzes exchanges within regions of shared *rrn* sequence identity. In discussing a model for *rrn* duplication, we favor the idea that DNA breaks often occur within the transcribed *rrn* region and produce gaps or breaks that can initiate duplications by two alternative pathways.

Duplication rates are strongly reduced in strains deficient for Holliday structure resolution

Standard pathways for homologous recombination (RecBC and RecFOR) involve early events that process breaks and gaps leading to RecA-catalyzed strand invasion. This produces Holliday junctions that are moved on recombining duplexes by RuvAB (Heller and Marians 2005; reviewed by West 2003). The later events that stabilize and ultimately resolve these Holliday structures are achieved by two alternative enzymes: (1) the RuvABC resolvase and (2) the RecG branch-migration enzyme (Benson *et al.* 1991; Wardrope and Leach 2009). If one resolution pathway is inactivated by mutation, the other is still available. Cells lacking both RuvC and RecG are severely deficient in recombination, presumably due to their inability to stabilize and resolve Holliday junctions. As seen in Figure 7, a *recG* mutation alone had little effect on duplication rate. The RecG enzyme is associated with the RecBCD pathway, which below we

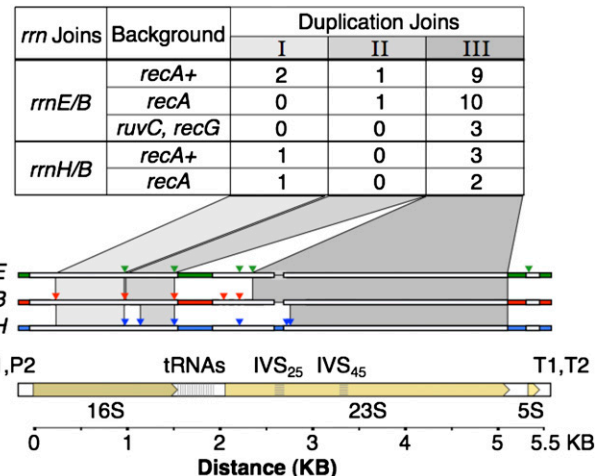


Figure 6 Exchange points within *rrn* loci that generate a *purHD* duplication. Exchange points all fell in regions of identical sequence (I, II, or III) shared by *rrnE* and *rrnB* and by *rrnH* and *rrnB*. These regions are shaded and are defined either by blocks of different sequences (white regions) or by single-nucleotide differences (colored triangles). The number of exchanges found in each interval are indicated in the table above the map. IVS₂₅ and IVS₄₅ are intervening sequences (like introns) that are found in some *rrn* loci of *Salmonella*, but not *E. coli* (Mattatall and Sanderson 1996). The 25 and 45 refer to helices in the secondary structure of the 23S rRNA. The distribution of these sequences among *rrn* loci is described in the Appendix.

argue does not contribute to duplication. Strains with a single *ruvAB* or *ruvC* mutation caused a significant drop in duplication rate. The largest decrease was seen in the *ruvC, recG* double mutant, which showed a 30-fold drop in duplication rate compared to that of wild type. This suggests that *rrn*-mediated duplications form by a recombination process that involves Holliday structures and requires their resolution by either RuvC or RecG. Of the residual duplications that formed at a reduced rate in the *ruvC recG* mutant, three junctions were sequenced and showed *rrnE/B* exchanges within the *rrn* sequence (see Figure 6), suggesting formation by single-strand annealing. The importance of Holliday structure resolution to duplication formation suggests that homologous recombination is normally involved in duplication formation despite the failure of *recA*, *-B*, or *-F* mutations to reduce the duplication formation rate. In addition to blocking recombination, the *ruvC recG* mutations may cause toxic accumulation of Holliday structures as seen previously in *Neisseria* (Sechman *et al.* 2006) and yeast (Fabre *et al.* 2002). This possibility will be discussed later.

Defects in early homologous recombination steps restore normal duplication rates to *ruvC recG* mutants

It was surprising that single *recA*, *-B*, and *-F* mutations and even a *recB, recF* double mutation, which block early steps in recombination, failed to affect a process that requires the late step of Holliday structure resolution. We expected a single *recB* or *recF* mutation to cause a less severe drop than a *recA* or a *recB, recF* double mutant. To pursue this, these early mutations were added to a *ruvC, recG* strain, defective

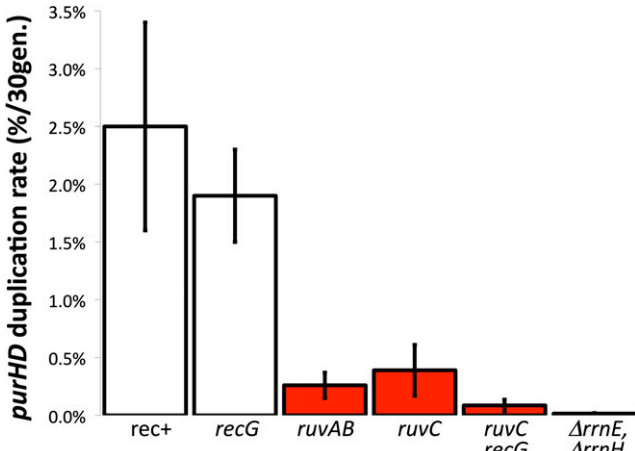


Figure 7 Duplication rate is reduced in strains defective in Holliday structure resolution. The duplication rate is defined as the frequency of duplications attained after 33 generations of growth. Bars in red indicate strains that showed a significant reduction in duplication rate. The bar at the far right indicates the rate in a strain lacking both *rrnE* and *rrnH*, both of which lie on the clockwise side of the assayed *purHD* operon.

for duplication. As seen in Figure 8, each of the single mutations restored a normal duplication rate. Thus, duplications of *purHD* formed at normal rates in strains lacking all of these major players in homologous recombination: RecA, RecB, RecF, RuvC, and RecG.

To explain the normal duplication rate in the suppressed *ruvC recG* mutants, we suggest that blockage of early recombination steps activates an alternative pathway that can form duplications by single-strand annealing and does not require RuvC or RecG. That is, duplications may form by homologous recombination in wild-type strains (despite the phenotypes seen in Figure 5). However, blockage of early recombination steps allows gaps and breaks to accumulate and provides ends that can form a duplication by single-strand annealing without need for strand invasion or Holliday structure resolution. When Holliday resolution is blocked, recombination cannot be completed, but the annealing pathway opened by early mutations supports duplication by an alternative annealing route for which Holliday resolution is irrelevant. A curious aspect of this suppression is that individual *recB*, *recF*, and *recA* mutations restored duplication. One might have expected that *recA* or the *recB*, *recF* mutation combination would be more effective than the *recB* or *recF* mutations individually. An explanation is suggested below.

Duplication by single-strand annealing raises a mechanistic problem. While it is easy to visualize use of an annealing pathway to form a deletion using resected ends at a chromosome break, formation of a duplication from one break would seem to require separation of strands for the entire duplicated region. Duplication by annealing is easier to imagine with two breaks, one near each participating *rrn* locus in different sister chromosomes. Because of frequent DNA breakage in *rrn* loci, delays in their repair caused by a *recA* (or *recF* or *recB*) mutation could allow damage to

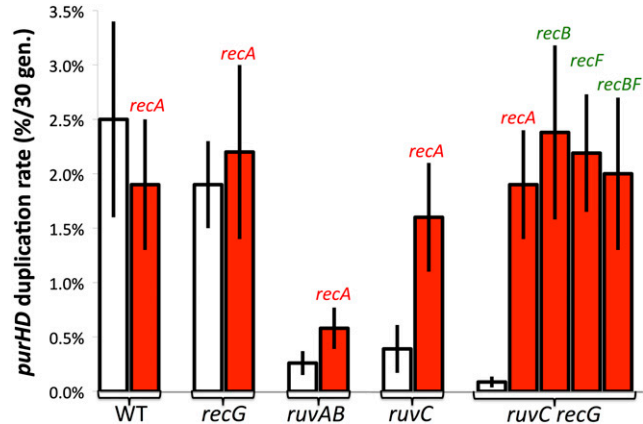


Figure 8 The duplication defect of *ruvC recG* is corrected by mutations in *recA*, *-B*, or *-F*. Duplication rates are the frequency of *purHD* duplications achieved by growing a cell lacking a duplication for 33 generations. White bars indicate the frequency in *recA*+ strains carrying the indicated mutations. Red bars indicate the frequency in the same strains with an added *recA*, *recB*, or *recF* mutation.

accumulate and assure coexistence of breaks in different *rrn* loci.

We suggest that, in the simple *ruvC recG* mutant, the early recombination functions (RecFORA and RecBCDA) continue to consume gaps and breaks that might otherwise provide ends for single-strand annealing. These early pathways try repeatedly but unsuccessfully to convert initial substrates into resolvable Holliday structures. Ultimately, these attempts may lead to loss of *rrn* sequences from the processed ends and thereby abort attempts at duplication. When RecA or the proteins that load RecA onto single strands (RecB or RecF) are eliminated, gaps and breaks remain unrepaired and can provide single-strand ends for use in annealing. These strands will not be coated with RecA protein and thus may be particularly active in annealing. In addition, these early blocks cause unrepaired gaps and breaks to accumulate, increasing the probability of non-allelic *rrn* loci in different sister chromosomes having simultaneous gaps or breaks. These simultaneous lesions may be essential to duplication formation by annealing as described below. The early blocks in recombination could also reduce any toxic effects of accumulated Holliday structures (see below).

The model described above is diagrammed in Figure 9 as it applies to duplication initiated by gaps. The gap may be generated by digesting one end of a nick or could be formed in one step following cutting of a hairpin structure in the nontranscribed strand of the *rrn* sequence (Figure 9, left). The RecFORA pathway starts repair of this gap using a sequence from a different *rrn* locus and generates Holliday structures that must be resolved by RuvC and RecG to complete recombinational duplication. When a *recF* mutation blocks early steps in gap repair, the gaps persist and accumulate such that two participating *rrn* loci can have single-strand ends with *rrn* sequences that can anneal (Figure 9, right). The annealing pathway activated by loss of gap

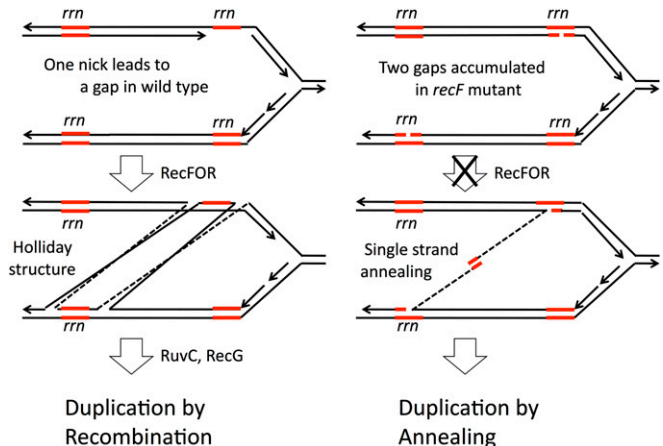


Figure 9 Formation of duplications at gaps by RecFORA recombination and by annealing in *recF* mutants. The model assumes that duplications are normally made primarily by the RecFORA pathway and are initiated by nicks within the *rrn* sequence. Strand exchange leads to Holliday structures that can be resolved to produce a duplication (left). In the absence of RecFORA, unrepaired nicks and gaps accumulate in both *rrn* cistrons and can produce single strands that are uncoated by RecA and available for formation of duplications by single-strand annealing (right). Activation of this pathway by *recF* mutation renders the RuvC and RecG enzymes dispensable and allows suppression of a *rvuC*, *recG* double mutation.

repair (the *recF* mutation) replaces the lost recombinational duplication pathway and explains why *recF* mutants showed no duplication defect (Figure 5). This activated pathway also suppresses the defect seen in a *rvuC* *recG* double mutant, since the new pathway does not involve Holliday structures. This model does not explain why single *recF* or *recB* mutations did not show some partial loss of duplication ability or partial suppression of *rvuC*, *recG*. To approach this, we looked for reasons that one kind of damage (perhaps double-strand breaks) might be prevented from making duplications.

All seven *rrn* loci are devoid of Chi sites

One aspect of the results in Figure 8 does not fit with the model as described above. It seemed reasonable that blockage of both RecFORA and RecBCDA pathways might be required to fully suppress the RuvC RecG defect. In fact, duplication rates were fully restored to the *rvuC* *recG* mutant by either a *recB* or a *recF* mutation individually. This could indicate that RecB and RecF act together to generate the Holliday structure. However, an alternative explanation was suggested by examining the sequences of *rrn* loci.

Chi sites are required for RecBCD-mediated homologous recombination. Repair of a double-strand break by RecBCD involves degrading double-stranded DNA until a Chi sequence is reached (reviewed by Kreuzer 2005 and by Myers and Stahl 1994). At this point, only the 5' end is further resected, leaving a 3' overhang ending at the point Chi was encountered. A break within or immediately origin-distal to the *rrn* sequence could generate an exchange between non-allelic *rrn* sequences only if Chi sites were present within the

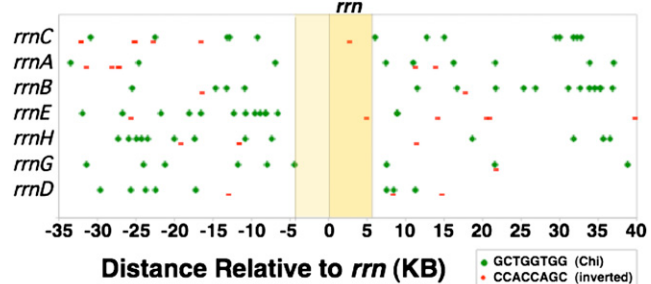


Figure 10 Distribution of Chi sites in and near *rrn* loci. The seven *rrn* sequences (5.5 kb) are aligned with each other, leaving 35 kb of sequences on either side of *rrn* that are completely different for each locus. In the diagram, large green dots indicate Chi sequences oriented to activate a RecBCD enzyme moving toward the replication origin (right to left). Smaller red bars indicate Chi sequences in the opposite orientation.

rrn locus. Figure 10 shows the positions of all Chi sequences in the 75-kb regions surrounding each of the seven *rrn* loci of *S. enterica*. It is apparent that Chi sites in the useful orientation are absent from all seven *rrn* loci and from all of their immediate origin-proximal 5-kb regions. Our calculations suggest that, given the frequency of Chi within the seven pictured regions (each 75 kb), the random chance of all *rrn* loci lacking Chi is ~0.5% and the probability of having no Chi sites in either the *rrn* or the origin-proximal 5-kb regions is 3×10^{-5} .

This Chi distribution suggests that, whenever RecBCD acts on a break within *rrn* sequences, it digests *rrn* material and produces a 3' end that can initiate an exchange only outside of *rrn*. In the absence of Chi sequences, RecBCD can still repair DNA breaks occurring within the *rrn* region but does so by exchanges outside of the *rrn* sequence. With no Chi sites within *rrn* loci, double-strand breaks cannot initiate RecBCD-mediated duplications or deletions, which require a recombination exchange between the *rrn* sequences of two different *rrn* loci. Data in Figure 6 (above) show that all of the duplications analyzed did arise by exchanges within the *rrn* sequence. This suggests that RecBCD activity at double-strand breaks could not be responsible for duplications arising in wild-type strains. This explains why a single *recB* mutation did not reduce the normal duplication rate—RecBCD does not contribute to duplication. Any duplications made by recombination must reflect the activity of RecFORA at gaps. However, the ability of a *recB* mutation to fully suppress the *rvuC* *recG* mutations must be explained.

The processing of double-strand breaks within *rrn* is diagrammed in Figure 11. In a normal strain (top left) the break can be repaired by RecBCD, but the process removes the *rrn* sequence adjacent to the break and leads to an exchange point outside of *rrn*, allowing repair of the break, but no contribution to duplication. In the absence of RecBCD, breaks accumulate and different *rrn* loci can provide ends for single-strand annealing. In a simple *recB* mutant, this additional annealing makes only a small contribution to duplication rate above the background of recombinational

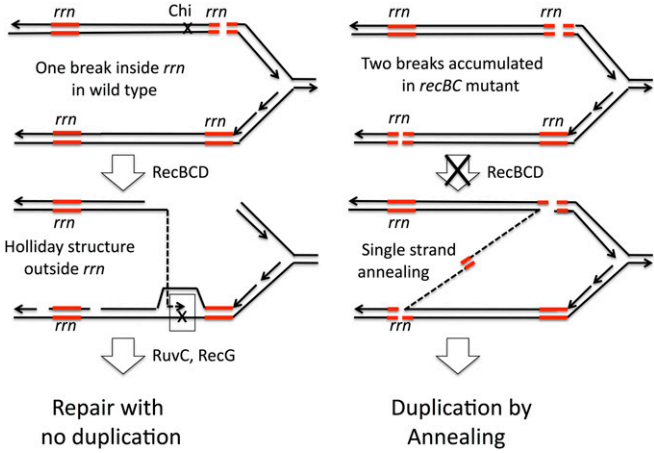


Figure 11 Repair of *rrn* double-strand breaks and effect of a *recB* mutation on duplication formation. Breaks within an *rrn* locus are subject to repair by RecBCD, which can restore a replication fork. However, the absence of Chi sequences within *rrn* loci prevents RecBCD from making exchanges between paralogous *rrn* loci (left). In the absence of RecBCD, breaks are not resected and can provide ends with *rrn* sequence. The resulting single-strand *rrn* sequences are free of RecA protein and can engage in single-strand annealing with non-allelic *rrn* sequences.

duplication by gap repair. However, when late steps in recombination are blocked in a *rvuC recG* double mutant, the *recB* mutation makes a large contribution to duplication rate by allowing double-strand breaks to provide ends that initiate annealing. That is, the *recB* mutation opens a new annealing pathway that uses double-strand breaks within *rrn* as initiating structures. Such structures could not contribute in any RecBCD-proficient situation (wild type, *recF*, or *recA*) and make a small contribution in any background that already has an active pathway for duplication gap repair by either recombination or annealing.

Thus, there may be three ways of making an *rrn* duplication. 1) Gaps can initiate recombinational duplication (using RecFORA) in wild type. 2) Gaps can initiate duplication by annealing in *recF* or *recA* cells. 3) Double-strand breaks can initiate annealing only in *recB* mutants. By allowing use of a new initiating structure, a *recB* mutation might be expected to increase the duplication rate over that seen either in wild type or in *recA* or *recF* mutants. This makes a prediction that is tested below with mixed results.

Duplication rate is stimulated slightly by *recB* mutation

In the process of duplication suggested above, *purHD* duplications arise in *rec⁺* strains predominantly by homologous recombination (RecFOR acting at gaps) and form exclusively by single-strand annealing in *recA* or *recF* mutants. Double-strand breaks within *rrn* cannot initiate duplications by recombination (using RecBCD), but do initiate annealing in *recB* mutants because *rrn* sequences are left at the unresected break. The increased annealing allowed by a *recB* mutation under some circumstances should increase the rate of duplication formation. In a strain that has functional RecFORA, the effect of the *recB* mutation would likely be small, since it

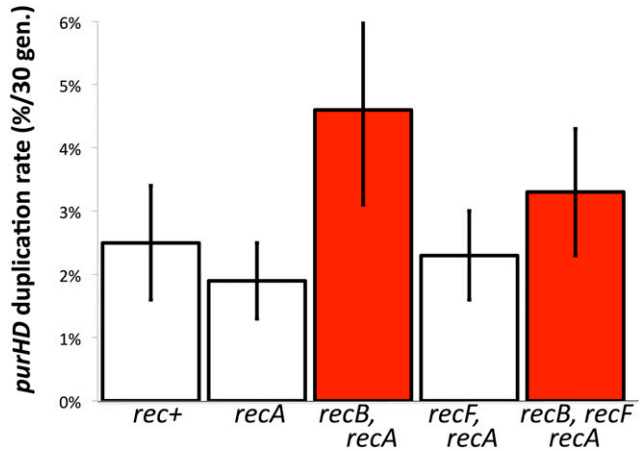


Figure 12 Duplication rates are stimulated by *recB* mutations in a *recA* mutant strain. Addition of a *recB* mutation causes a small increase in the *purHD* duplication rate in strains lacking *recA*. In *recA* mutants, duplications may form entirely by single-strand annealing. Absence of RecB may leave undigested *rrn* sequences at double-strand breaks, enhancing the likelihood of duplication by annealing.

would enhance an already high rate of duplications due to RecFORA acting at gaps. Similarly, the enhancement might be small in a *recF* mutant because gaps provide a good source of duplication by annealing. The magnitude of duplication enhancement provided by a *recB* mutation would depend on the relative frequency of gaps and breaks. We have looked for evidence of this enhancement.

The *recB* mutation shows no significant enhancement in Figure 5, in wild type (above a background of gap-stimulated recombination), or in a *recF* strain (above a background of gap-initiated annealing). The increase in rate caused by *recB* in a *recF, recA* background does not appear significant (Figure 12). However, a slight effect was seen in a *recA* mutant background (Figure 12). This difference is on the border of significance, given the variability of these measurements, but the duplication rate seen in the *recA, recB* double mutant is the highest that we have measured in any strain. This rate may reflect annealing initiated by both gaps and breaks.

Effects of mismatch repair on duplication formation

The seven *rrn* loci of *Salmonella* differ at many points in their sequence (see Figure 6 and Appendix). Since duplications form by exchanges between different *rrn* loci, it seemed possible that recombination or even annealing might be subject to rejection of duplexes by the methyl-directed mismatch repair system (MMR) (Petit *et al.* 1991; Friedberg *et al.* 2005). This idea is supported by the observation (Figure 13) that a *mutS* mutation stimulated duplication in the *recA⁺* background. No effect of *mutS* was seen in the *recA* mutant background, so we suggest that *rrn* heteroduplexes formed by single-strand annealing are not subject to MMR rejection. This result differs from earlier findings using shorter and more closely positioned repeats, for which MMR played a big role in annealing (Bzymek and Lovett 2001).

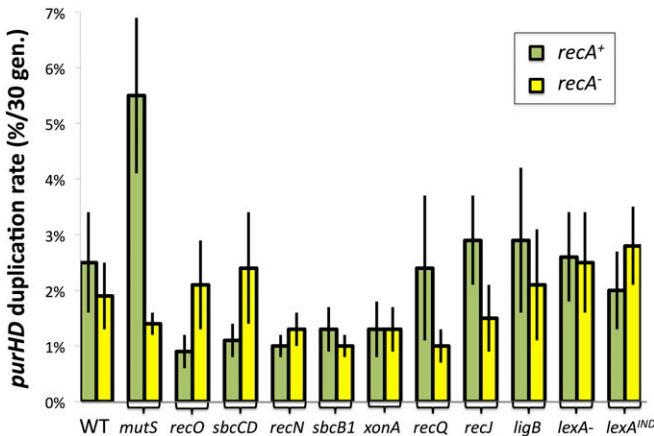


Figure 13 Effects of various mutations on duplication rates with and without RecA. Duplication rates were measured in *recA*⁺ (green bars) and *recA* (yellow bars) strains carrying additional mutations in genes involved in mismatch repair, recombination, SOS response, and, possibly, in single-strand annealing.

Testing the role of other recombination/repair functions in duplication

If duplications form efficiently by annealing in *recA* mutant strains, then mutations that inhibit annealing might decrease duplication rate in a *recA* mutant strain and might show no defect in *recA*⁺ strains, where duplications form primarily by homologous recombination. A series of mutations defective in various recombination and DNA repair functions were tested for their effect on duplication rates in *recA*⁺ and *recA*⁻ strains (see Figure 13). While these effects are too small to be interpreted, several seem interesting.

Most notable is the effect of *recO* mutations, which remove a central part of the gap repair mechanism (RecFORA). One might expect this mutation to behave as did the *recF* mutation described above. In a *recA*⁺ background, the *recO* mutation caused a significant drop in duplication rate, suggesting that it might eliminate the gap-initiated recombination that normally forms a duplication in a wild-type cell. The *recF* mutation (Figure 5) did not cause this drop, arguably because it activated the alternative annealing pathway. This might suggest that *recO* defects are less able to prevent loading of RecA on single strands and thus less able to activate annealing. In keeping with this idea, the *recO* mutation had no effect on duplication in a *recA* mutant, where no RecA protein is available to be loaded.

The *sbcCD* mutation caused a small reduction in duplication in an otherwise *rec*⁺ strain but not in a *recA* mutant. SbcCD degrades hairpin structures in single-strand DNA (Eykelboom *et al.* 2008; Darmon *et al.* 2010) and might be expected to contribute to creation of gaps in ribosomal DNA (rDNA). Large gaps could be particularly important for recombination, which requires RecA loading, while smaller gaps are sufficient for annealing in a *recA* mutant where the only ends are needed and RecA loading is not an issue.

The *sbcB* and *xonA* mutations (dominant and null alleles of the gene for a 3' exonuclease *ExoI*) may cause a small

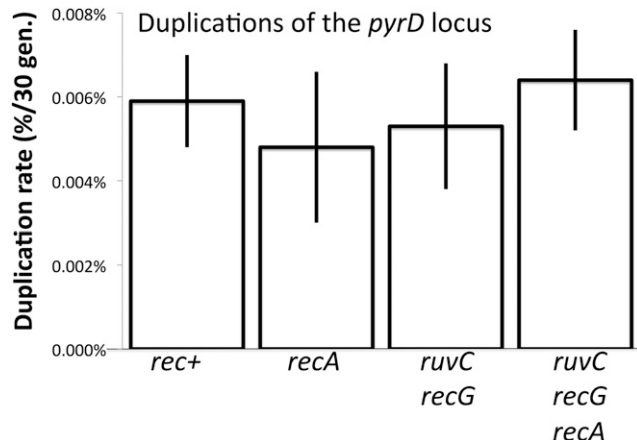


Figure 14 Effect of recombination defects on *pyrD* duplications. The *pyrD* locus is located far from the *purHD* site (see Figure 2) and is not flanked by direct-order *rrn* loci or by any other major sequence repeat.

decrease in both pathways. *ExoI* and the RecJ single-strand 5' exonuclease could be imagined to contribute by extending single-strand nicks to gaps, but *recJ* mutations showed little effect on duplication rate. The *ligB* gene encodes a non-essential homolog of the standard DNA ligase (*ligA*) (Sriskanda and Shuman 2001) and made no significant contribution to duplication formation.

There was also very little effect of *lexA^{Null}* and *lexA^{Ind}* mutations, which cause the LexA-repressed SOS DNA repair system to be either constitutively expressed or uninducible, respectively. The same result applied to both *recA*⁺ and *recA* strains. This suggests that none of the 40 enzymes controlled by the SOS response is limiting for *rrn*-mediated duplication by either recombination or annealing (Friedberg *et al.* 2005).

ruvC recG mutation combination does not affect duplication rate of the distant *pyrD* locus

The dependencies described above apply to duplications of the *purHD* locus, which is flanked by *rrn* loci. In contrast, the *pyrD* gene is located on the opposite side of the chromosome (see Figure 2) and is not closely flanked by *rrn* or any other major direct-order sequence repeats. The *pyrD* duplication rate is the lowest of all *Salmonella* loci tested at 4×10^{-6} /cell/generation, 750-fold lower than the rate for *rrn*-mediated duplication of *purHD* (Reams *et al.* 2010). The *pyrD* duplication rate is unaffected by a *recA* mutation (like that of *purHD* locus). Unlike *purHD*, the *pyrD* locus duplicates at a normal rate in *ruvC*, *recG* mutants (see Figure 14).

In understanding the different effects of Holliday resolution in these two regions, it should be noted that these loci duplicate at very different rates (10^{-6} for *pyrD* and 10^{-3} for *purHD*). In addition, the *pyrD* locus is not flanked by extensive sequence repeats while *purHD* is closely flanked by the *rrnB* and *rrnE* loci. These differences suggest that *pyrD* normally duplicates by pathways that are independent of RecA and involve no Holliday structures (or RuvC, RecG activity). These duplications must use the very short available homologies,

which has been verified by sequencing junctions of *pyrD* duplications (E. Kofoid, unpublished results). It seems likely that *pyrD* duplicates (at a low rate) by nonrecombination pathways that use single-strand annealing or the palindrome-processing pathway described previously for tandem inversion duplications (TIDs) (Kugelberg *et al.* 2006) and discussed below. While the duplication rate of *pyrD* is very low, this behavior seems likely to be representative of most areas of the chromosome, which have no flanking extensive sequence repeats and no mechanisms to stimulate formation of gaps or breaks. A *purHD* from which the repeated *rrnB* and *rrnH* loci were deleted behaved much like *pyrD*. Without flanking *rrn* repeats, the *purHD* duplication rate falls 100-fold (see Table 2) and is no longer affected by *rvuC*, *recG* mutations (A. Reams, unpublished results).

Discussion

Three unexpected results are described here. First, formation rates of duplications arising between extensive repeated *rrn* sequences are unaffected by the absence of enzymes essential for homologous recombination (RecA, RecB, and RecF). Second, while strains lacking these early recombination functions form duplications at normal rates, mutants (*rvuC* *recG*) blocked for late recombination steps (Holliday structure resolution) show a 30-fold decrease in duplication rates. Third, the reduced duplication rates seen in the absence of RuvC and RecG are corrected by single blocks in earlier steps of homologous recombination (RecA, RecB, or RecF). These observations may reflect shifts in channeling a rich source of gaps and breaks between two alternative pathways of duplication formation–recombination and single-strand annealing.

In many assay systems, duplications mediated by large direct repeats depend heavily on RecA (Romero and Palacios 1997). However, these assays detect duplications by positive selections that demand multiple gene copies and may favor cells with higher amplifications. Since the amplification of a duplication to higher copy numbers is heavily RecA dependent (Kugelberg *et al.* 2006, 2010; Poteete 2009; Reams *et al.* 2010), we suspect that the frequently reported RecA dependency of duplication reported in other systems may reflect a need for higher amplification, which can depend on RecA even when the initial duplication event is RecA independent. The assay used here traps duplications without favoring higher copy numbers. In addition, this assay is not affected by the lethal effects of recombination mutations tested. That is, reduced viability of certain mutant strains (e.g., *recA*, *rvuC*) does not lower the measured duplication rate since the trapping assay detects the ratio of duplication to nonduplication cells in the viable population.

A different but not mutually exclusive explanation for the RecA independence of *rrn*-mediated duplications is that the repeated *rrn* sequences may be subject to frequent formation of gaps and breaks. A precedent for the role of introduced breaks may be the low recombination dependence of duplications between IS3 elements, which depend on the

availability of transposase to make nicks in the two recombining sequences (Reams *et al.* 2012). Nicks and/or breaks in both recombining sequences can allow accumulation of the multiple simultaneous breaks needed for duplication by single-strand annealing and allow duplications to form without recombination. When these lesions are not processed by recombinational repair enzymes, they may be free to initiate an alternative annealing pathway for duplication formation.

The 5.5-kb *rrn* repeats are heavily transcribed and rich in palindromic sequences. These genes are GC-rich and GC-skewed such that the nontranscribed strand is G-rich and may be subject to formation of R-loops with hairpin structures. In *Salmonella*, several *rrn* sequences have extended palindromic intervening sequences (IVS in Figure 6) that extend natural palindromes that are inherent in the ribosomal RNA (rRNA) sequences. These extensions must be cut out of rRNA prior to ribosome assembly (Mattatall and Sanderson 1996, 1998). The distribution of these palindromic sequences among various *rrn* loci is described in the Appendix. Degradation of hairpin structures in the nontranscribed strand of rDNA would generate gaps in one step. The heavy transcription of *rrn* regions may temporarily expose single strands, making them available for pairing and susceptible to nucleases. The heavy transcription of *rrn* loci is likely to require activity of topoisomerases and gyrases, which, we speculate, may cause a significant rate of DNA breakage. These enzymes are able to catalyze illegitimate recombination (Ikeda *et al.* 1982) and make double-strand breaks in the presence of inhibitors or following collisions with replication forks (Gellert *et al.* 1977; Pohlhaus and Kreuzer 2005). While the frequent breakage of *rrn* sequences is speculative, it should be remembered that *rrn* duplications form at a very high frequency (10^{-3} /cell/generation) and end in specific short regions (5.5 kb), suggesting a need for frequent internal initiating structures.

A model for formation of *rrn* duplications

We propose that the results described above are consistent with the idea that *rrn* loci are subject to frequent nicks and breaks that can be processed in alternative ways and form duplications by the several pathways described below.

1. In wild-type strains, duplications are made primarily by homologous recombination between sister strands using the RecFORA pathway (see Figure 9, left). Single-strand gaps within *rrn* sequences are loaded with RecA protein and invade a non-allelic *rrn* sequence of a sister chromosome, thereby generating Holliday structures that can be resolved to leave a duplication.
2. Elimination of the RecFORA pathway prevents recombinational formation of duplications, but allows unrepaired gaps to accumulate in both participating *rrn* loci. These gaps provide ends that can participate in an alternative single-strand annealing pathway (see Figure 9, right). The absence of RecA or failure to load RecA onto the

gaps leaves single-strand ends free to engage in single-strand annealing. Evidence that RecA inhibits annealing was previously reported in *E. coli* (Bzymek and Lovett 2001), and the yeast RecA homolog Rad51 also inhibits single-strand annealing (McDonald and Rothstein 1994; Ivanov *et al.* 1996; Stark *et al.* 2004).

3. Double-strand breaks within *rrn* loci cannot initiate duplications because Chi sites are absent from all *rrn* loci (see Figure 10). Repair of *rrn* breaks by RecBCD is expected to occur by exchanges outside of *rrn* (Figure 11, left). Thus, a *recB* mutant shows no loss of duplication rate.
4. In a *rvuC recG* mutant, recombination is blocked by inability to resolve Holliday structures. (see Figure 9, left). In this mutant, however, the RecFORA enzymes continue to convert gaps into unresolvable Holliday structures. By processing gaps that might have led to annealing, the active RecFORA functions block the alternative annealing route to duplication. Repeated attempts to establish Holliday structures may ultimately lead to loss of *rrn* sequences from ends and thus prevent *rrn* rearrangements. The few *rrn* duplications formed in a *rvuC recG* mutant form by exchanges within *rrn* like those thought to form by annealing. The possibility of toxic Holliday structures is discussed below.
5. When *recA* or *recF* mutations are added to a *rvuC recG* mutant, gaps are allowed to accumulate and open the compensating annealing pathway, just as was seen in strains with only a *recA* or *recF* mutation. Thus, in the absence of these early recombination steps, single-strand annealing is stimulated and RuvC and RecG functions become irrelevant since there is no way to make a Holliday structure.
6. Addition of a *recB* mutation to a *rvuC recG* double mutant prevents digestion of *rrn* sequence from double-strand breaks within *rrn* and allows double-strand ends to initiate duplication by annealing. Thus, double-strand breaks within *rrn*, which do not normally contribute to recombinational duplication (due to lack of Chi), can contribute to duplication by annealing in the absence of RecBCD degradation.

A remarkable aspect of the reported results is that a similar rate of duplication was seen regardless of the pathway used. If the activated annealing pathway makes up for a loss in recombination events and leaves the duplication rate largely unchanged, the two pathways must function at the same rate. Similarly, when a *recB* mutation is added to a *rvuC, recG* mutant, the final rate is very similar to that seen in wild type, in *recA*, or in *recF*. We suggest that the similarity in rates reflects dependence on a limiting resource, the gaps and breaks that initiate the exchange, regardless of the pathway used. That is, gaps form at a limiting rate and are essentially all ultimately repaired by either one pathway or the other. The similarity of rates when double-strand annealing is allowed by a *recB* mutation may suggest that the rate

of forming breaks within *rrn* is equivalent or a bit lower to that of forming gaps. It should be kept in mind that the exchange events measured here arise at a very high rate— 10^{-3} /cell/division.

Requirements for activation of annealing pathways

This model suggests that normal recombination functions not only contribute to duplication by homologous recombination, but also minimize the likelihood of single-strand annealing by processing structures such as nicks or gaps and coating single strands with RecA protein. This inhibition may minimize rearrangements between long direct repeats that are prone to frequent damage, such as *rrn* sequences. The model also suggests that annealing can be initiated either by single-strand nicks and gaps or by double-strand breaks. In the case of *rrn* loci, formation of these lesions may be stimulated by the high transcription rate and abundance of included palindromic sequences. A previous report on *E. coli* has shown that deletions arising by single-strand annealing are strongly enhanced by intervening palindromes (Bzymek and Lovett 2001).

The ability of recombination pathways to block rearrangement by annealing may also involve coating single strands with RecA protein. Coated single strands (*i.e.*, RecA filaments) are impaired for annealing. Evidence for the stimulation of single-strand annealing by the absence of a functional RecA has been previously reported in *E. coli* (Bzymek and Lovett 2001). The activation of the annealing pathway may require elimination of RecA or the proteins that load RecA onto a single strand (*i.e.*, RecFOR or RecBCD). This fits with a *recF* mutant, which can accumulate unrepaired nicks and gaps as outlined above, and also fails to load RecA on single-strand regions. Similarly, a *recB* mutant fails to remove *rrn* sequence from ends at a break and also fails to load RecA onto single-strand ends.

While the genes involved in homologous recombination have been studied extensively in *E. coli* and *Salmonella*, relatively very little is known about the annealing process. Several proteins have been associated with single-strand annealing in bacteria, including SbcCD (Bzymek and Lovett 2001; Goldfless *et al.* 2006). Figure 11 shows the effects of removing these functions from a *recA* mutant strain, in which duplications are believed to arise exclusively by annealing (Figure 13). Of the enzymes tested, only *recQ* and *recJ* mutations appeared to reduce duplication by annealing, but their effect was small. No effect was seen for SbcCD, although this nuclease might have been expected to cut palindromic structures in *rrn* genes and contribute to initiation by both pathways (Connelly *et al.* 1998). Duplication formation in a wild-type strain, presumed to involve RecA, was stimulated by a mismatch-repair defect (*mutS*), suggesting rejection of mismatched heteroduplexes, whereas the RecA-independent annealing pathway was unaffected. These results are consistent with the idea that *rrn*-mediated duplications arise by two alternative pathways, each dependent on different sets of genetic components.

Lethal effects of accumulated Holliday structures

The *rvuC* *recG* mutation combination is known to severely reduce recombination rates and lowers cell viability to 20% in an overnight culture of *E. coli* (Lloyd 1991). Recently, lethality has been attributed to the toxic effects of a failure to resolve Holliday structures in both yeast (Fabre *et al.* 2002) and *Neisseria* (Sechman *et al.* 2006). The general loss of viability in *E. coli* *rvuC* *recG* mutants is thus likely to reflect toxic Holliday structures formed by sister-strand exchanges following occasional spontaneous damage. This general loss of viability is not likely be responsible for the reduced duplication rate described here (Figure 7 and Figure 8) because the measured duplication rate is based on the relative frequency of cells with and without a duplication, which are subject to the same loss of viability. However, it is possible that the 30-fold drop in duplication rate is associated with lethal effects of Holliday structures formed in the course of recombination between *rrn* loci. That is, *rvuC* and *recG* mutations block recombination between *rrn* sequences and cause accumulation of a lethal intermediate. Such lethality is specific to the production of *rrn* duplications, but is peripheral to the general model presented here as long as it requires *rrn-rrn* recombination and duplication would be prevented with or without the lethal effect. The *recA*, *recB*, and *recF* mutations that suppress *rvuC*, *recG* not only allow initiating structures to accumulate and activate an annealing pathway, but also prevent formation of toxic Holliday structures. In *Neisseria*, pilin variation is achieved by recombination between an expression site and silent copies of the pilin gene (Sechman *et al.* 2006). These exchanges are lethal in strains unable to resolve Holliday structures, and lethality requires both RecA and a mechanism to stimulate the exchange (Cahoon and Seifert 2011). Thus lethality seen in pilin variation and possibly in *rrn* recombination may reflect high exchange rates in specific restricted sequences.

Similarity to previously reported results for bacterial conjugation

A pattern of genetic dependencies similar to those reported here was seen previously for plasmid conjugation in *E. coli* (Benson *et al.* 1991). The conjugative F' lac⁺ plasmid is transferred between cells as a single strand, whose recombination with the chromosome is low. Acquisition of the plasmid is reduced in *rvu* mutants and this defect is corrected by an added *recA* mutation. These results suggest that plasmid circularization normally occurs by recombination requiring Holliday structure resolution, but removal of *recA* activates an alternative RecA-independent pathway that may involve annealing.

Comparing these results to previous studies of rDNA recombination in yeast

In budding yeast, *rrn* loci are present as a tandem array of >100 identical copies of a 9-kb repeat, in which copy

number is subject to frequent change (Linskens and Huberman 1988). Duplication of an rDNA sequence has been attributed to gene conversion rather than unequal recombination because addition of a copy is seldom accompanied by a corresponding deletion. That is, the exchange that generates a duplication is usually nonreciprocal (Gangloff *et al.* 1996). While standard conversion events would be expected to require canonical recombination functions, the rate of rDNA copy-number increase is not reduced by lack of Rad51, Rad52, or Rad59 (Houseley and Tollervey 2011). Although the process of yeast rDNA copy-number control is complex (Fierro 1999; Pâques and Haber 1999), it may resemble the process described here in that copy-number changes are caused by homologous recombination, but can also arise by alternative annealing pathways that are activated when recombination is prevented. In addition, the copy-number changes in yeast rDNA copies may be more similar to the second step of amplification (e.g., increasing from a tandem duplication to three tandem copies). In bacteria, multiple, closely positioned substantial repeats interact to cause copy-number changes by a process that is highly RecA dependent. In contrast, the *de novo* bacterial *rrn* duplications described here involve interactions between two separate imperfect repeats that are highly transcribed and have the potential to form secondary structures.

Alternatives to duplication by the single-strand-annealing pathway

Single-strand annealing is proposed as the RecA-independent alternative pathway for duplication formation. Annealing avoids the need for strand invasion, but requires simultaneous breaks or nicks to generate single strand from different *rrn* sequences. A completely different RecA-independent duplication pathway has been proposed to explain the origin of short duplications that amplify during growth under selection in the Cairns system (Cairns and Foster 1991; Roth *et al.* 2006). In this pathway, a quasi-palindromic sequence initiates repair replication from a snap-back structure that eventually switches template strands, perhaps stimulated by a second palindrome, to make three copies of the intervening region (Kugelberg *et al.* 2010). The resulting triplication has direct-order copies flanking a central inverse order copy—a symmetrical tandem inversion duplication (sTID). The two internal quasi-palindromic sTID junctions are prone to deletions because of their propensity to form secondary hairpin structures. Such structures, singly or together, can be deleted to leave a TID with asymmetric junctions or a simple direct repeat duplication. The first step of this pathway has been clearly demonstrated by Leach and coworkers (Darmon *et al.* 2010), and palindromes have been shown to stimulate deletion formation in several systems (Sinden *et al.* 1991; Bzymek and Lovett 2001).

Palindrome processing by the TID pathway is attractive for *rrn* duplications because palindromes within the locus could be used for both initiation and strand switching. However, the large duplicated regions, such as *rrnB-rrnH* (790

kb), would necessitate repair synthesis of extensive chromosomal regions. Observed TID amplifications are generally shorter (10–30 kb) (Araya *et al.* 2010; Kugelberg *et al.* 2010). Palindrome processing also does not easily explain the reduced duplication rate seen in a *rvuC recG* double mutant. While the TID mechanism remains a formally possible way to form *rrn* duplications, we suggest that this pathway is more likely to apply to the RecA-independent duplications that arise at low rates in regions without long direct-order flanking repeats.

Acknowledgments

We thank Sophie Maisnier-Patin, John Paul Aboubechara, Semarhy Quinones-Soto, Douglas Huseby, Wolf Heyer and Steven Kowalczykowski for helpful suggestions. This work was supported by National Institutes of Health grant GM27068.

Literature Cited

Anderson, P., and J. Roth, 1981 Spontaneous tandem genetic duplications in *Salmonella typhimurium* arise by unequal recombination between rRNA (*rrn*) cistrons. *Proc. Natl. Acad. Sci. USA* 78: 3113–3117.

Araya, C. L., C. Payen, M. J. Dunham, and S. Fields, 2010 Whole-genome sequencing of a laboratory-evolved yeast strain. *BMC Genomics* 11: 88.

Benson, F., S. Collier, and R. G. Lloyd, 1991 Evidence of abortive recombination in *rvu* mutants of *Escherichia coli* K12. *Mol. Gen. Genet.* 225: 266–272.

Bzymek, M., and S. T. Lovett, 2001 Evidence for two mechanisms of palindrome-stimulated deletion in *Escherichia coli*: single-strand annealing and replication slipped mispairing. *Genetics* 158: 527–540.

Cahoon, L. A., and H. S. Seifert, 2011 Focusing homologous recombination: pilin antigenic variation in the pathogenic *Neisseria*. *Mol. Microbiol.* 81: 1136–1143.

Cahoon, L. A., and H. S. Seifert, 2013 Transcription of a cis-acting, noncoding, small RNA is required for pilin antigenic variation in *Neisseria gonorrhoeae*. *PLoS Pathog.* 9: e1003074.

Cairns, J., and P. L. Foster, 1991 Adaptive reversion of a frameshift mutation in *Escherichia coli*. *Genetics* 128: 695–701.

Connelly, J. C., L. A. Kirkham, and D. R. Leach, 1998 The SbcCD nuclease of *Escherichia coli* is a structural maintenance of chromosomes (SMC) family protein that cleaves hairpin DNA. *Proc. Natl. Acad. Sci. USA* 95: 7969–7974.

Court, D. L., J. A. Sawitzke, and L. C. Thomason, 2002 Genetic engineering using homologous recombination. *Annu. Rev. Genet.* 36: 361–388.

Darmon, E., J. K. Eykelenboom, F. Lincker, L. H. Jones, M. White *et al.*, 2010 *E. coli* SbcCD and RecA control chromosomal rearrangement induced by an interrupted palindrome. *Mol. Cell* 39: 59–70.

Dennis, P. P., M. Ehrenberg, and H. Bremer, 2004 Control of rRNA synthesis in *Escherichia coli*: a systems biology approach. *Microbiol. Mol. Biol. Rev.* 68: 639–668.

Eykelenboom, J. K., J. K. Blackwood, E. Okely, and D. R. Leach, 2008 SbcCD causes a double-strand break at a DNA palindrome in the *Escherichia coli* chromosome. *Mol. Cell* 29: 644–651.

Fabre, F., A. Chan, W. D. Heyer, and S. Gangloff, 2002 Alternate pathways involving Sgs1/Top3, Mus81/Mms4, and Srs2 prevent formation of toxic recombination intermediates from single-stranded gaps created by DNA replication. *Proc. Natl. Acad. Sci. USA* 99: 16887–16892.

Fierro, F. M. J., 1999 Molecular mechanisms of chromosomal rearrangement in fungi. *Crit. Rev. Microbiol.* 25: 1–17.

Friedberg, E. C., G. C. Walker, W. Siede, R. D. Wood, and A. Schultz, 2005 *DNA Repair and Mutagenesis*. ASM Press, Washington, DC.

Gangloff, S., H. Zou, and R. Rothstein, 1996 Gene conversion plays the major role in controlling the stability of large tandem repeats in yeast. *EMBO J.* 15: 1715–1725.

Gellert, M., K. Mizuchi, M. H. O'Dea, T. Itoh, and J. I. Tomizawa, 1977 Nalidixic acid resistance: a second genetic character involved in DNA gyrase activity. *Proc. Natl. Acad. Sci. USA* 74: 4772–4776.

Goldfless, S. J., A. S. Morag, K. A. Belisle, V. A. Sutera, Jr., and S. T. Lovett, 2006 DNA repeat rearrangements mediated by DnaK-dependent replication fork repair. *Mol. Cell* 21: 595–604.

Heller, R. C., and K. J. Marians, 2005 The disposition of nascent strands at stalled replication forks dictates the pathway of replisome loading during restart. *Mol. Cell* 17: 733–743.

Helm, R. A., and S. Maloy, 2001 Rapid approach to determine *rrn* arrangement in *Salmonella* serovars. *Appl. Environ. Microbiol.* 67: 3295–3298.

Helm, R. A., A. G. Lee, H. D. Christman, and S. Maloy, 2003 Genomic rearrangements at *rrn* operons in *Salmonella*. *Genetics* 165: 951–959.

Houseley, J., and D. Tollervey, 2011 Repeat expansion in the budding yeast ribosomal DNA can occur independently of the canonical homologous recombination machinery. *Nucleic Acids Res.* 39: 8778–8791.

Ikeda, H., K. Aoki, and A. Naito, 1982 Illegitimate recombination mediated in vitro by DNA gyrase of *Escherichia coli*: structure of recombinant DNA molecules. *Proc. Natl. Acad. Sci. USA* 79: 3724–3728.

Ivanov, E. L., N. Sugawara, J. Fishman-Lobell, and J. E. Haber, 1996 Genetic requirements for the single-strand annealing pathway of double-strand break repair in *Saccharomyces cerevisiae*. *Genetics* 142: 693–704.

Kreuzer, K. N., 2005 Interplay between DNA replication and recombination in prokaryotes. *Annu. Rev. Microbiol.* 59: 43–67.

Kugelberg, E., E. Kofoed, A. B. Reams, D. I. Andersson, and J. R. Roth, 2006 Multiple pathways of selected gene amplification during adaptive mutation. *Proc. Natl. Acad. Sci. USA* 103: 17319–17324.

Kugelberg, E., E. Kofoed, D. I. Andersson, Y. Lu, J. Mellor *et al.*, 2010 The tandem inversion duplication in *Salmonella enterica*: selection drives unstable precursors to final mutation types. *Genetics* 185: 65–80.

Linskens, M. H., and J. A. Huberman, 1988 Organization of replication of ribosomal DNA in *Saccharomyces cerevisiae*. *Mol. Cell. Biol.* 8: 4927–4935.

Liu, S. L., and K. E. Sanderson, 1998 Homologous recombination between *rrn* operons rearranges the chromosome in host-specialized species of *Salmonella*. *FEMS Microbiol. Lett.* 164: 275–281.

Lloyd, R. G., 1991 Conjugational recombination in resolvase-deficient *rvu* mutants of *Escherichia coli* K-12 depends on *recG*. *J. Bacteriol.* 173: 5414–5418.

Mattatall, N. R., and K. E. Sanderson, 1996 *Salmonella typhimurium* LT2 possesses three distinct 23S rRNA intervening sequences. *J. Bacteriol.* 178: 2272–2278.

Mattatall, N. R., and K. E. Sanderson, 1998 RNase III deficient *Salmonella typhimurium* LT2 contains intervening sequences (IVSs) in its 23S rRNA. *FEMS Microbiol. Lett.* 159: 179–185.

McDonald, J. P., and R. Rothstein, 1994 Unrepaired heteroduplex DNA in *Saccharomyces cerevisiae* is decreased in *RAD1* *RAD52*-independent recombination. *Genetics* 137: 393–405.

Myers, R. S., and F. W. Stahl, 1994 Chi and the RecBC D enzyme of *Escherichia coli*. *Annu. Rev. Genet.* 28: 49–70.

Pâques, F., and J. E. Haber, 1999 Multiple pathways of recombination induced by double-strand breaks in *Saccharomyces cerevisiae*. *Microbiol. Mol. Biol. Rev.* 63: 349–404.

Petit, M. A., J. Dimpfl, M. Radman, and H. Echols, 1991 Control of large chromosomal duplications in *Escherichia coli* by the mismatch repair system. *Genetics* 129: 327–332.

Pohlhaus, J. R., and K. N. Kreuzer, 2005 Norfloxacin-induced DNA gyrase cleavage complexes block *Escherichia coli* replication forks, causing double-stranded breaks in vivo. *Mol. Microbiol.* 56: 1416–1429.

Poteete, A. R., 2009 Expansion of a chromosomal repeat in *Escherichia coli*: roles of replication, repair, and recombination functions. *BMC Mol. Biol.* 10: 14.

Reams, A. B., and E. L. Neidle, 2003 Genome plasticity in *Acinetobacter*: new degradative capabilities acquired by the spontaneous amplification of large chromosomal segments. *Mol. Microbiol.* 47: 1291–1304.

Reams, A. B., and E. L. Neidle, 2004 Gene amplification involves site-specific short homology-independent illegitimate recombination in *Acinetobacter* sp. strain ADP1. *J. Mol. Biol.* 338: 643–656.

Reams, A. B., E. Kofoid, M. Savageau, and J. R. Roth, 2010 Duplication frequency in a population of *Salmonella enterica* rapidly approaches steady state with or without recombination. *Genetics* 184: 1077–1094.

Reams, A. B., E. Kofoid, E. Kugelberg, and J. R. Roth, 2012 Multiple pathways of duplication formation with and without recombination (RecA) in *Salmonella enterica*. *Genetics* 192: 397–415.

Romero, D., and R. Palacios, 1997 Gene amplification and genomic plasticity in prokaryotes. *Annu. Rev. Genet.* 31: 91–111.

Roth, J. R., N. Benson, T. Galitski, K. Haack, J. G. Lawrence *et al.*, 1996 Rearrangement of the bacterial chromosome: formation and applications, pp. 2256–2276 in *Escherichia coli and Salmonella*, edited by F. C. Neidhardt. ASM Press, Washington, DC.

Roth, J. R., E. Kugelberg, A. B. Reams, E. Kofoid, and D. I. Andersson, 2006 Origin of mutations under selection: the adaptive mutation controversy. *Annu. Rev. Microbiol.* 60: 477–501.

Sechman, E. V., K. A. Kline, and H. S. Seifert, 2006 Loss of both Holliday junction processing pathways is synthetically lethal in the presence of gonococcal pilin antigenic variation. *Mol. Microbiol.* 61: 185–193.

Sinden, R. R., G. X. Zheng, R. G. Brankamp, and K. N. Allen, 1991 On the deletion of inverted repeated DNA in *Escherichia coli*: effects of length, thermal stability, and cruciform formation in vivo. *Genetics* 129: 991–1005.

Sriskanda, V., and S. Shuman, 2001 A second NAD(+) -dependent DNA ligase (LigB) in *Escherichia coli*. *Nucleic Acids Res.* 29: 4930–4934.

Stark, J. M., A. J. Pierce, J. Oh, A. Pastink, and M. Jasin, 2004 Genetic steps of mammalian homologous repair with distinct mutagenic consequences. *Mol. Cell. Biol.* 24: 9305–9316.

Wardrope, L., E. O., and D. Leach, 2009 Resolution of joint molecules by RuvABC and RecG following cleavage of the *Escherichia coli* chromosome by EcoKI. *PLoS ONE* 4: e6542.

West, S. C., 2003 Molecular views of recombination proteins and their control. *Nat. Rev. Mol. Cell Biol.* 4: 435–445.

Communicating editor: S. Sandler

Appendix: Sequence Differences Between *rrn* Loci in *Salmonella enterica*

The figure below describes the sequence variation between the seven *rrn* loci of *S. enterica*. The central cluster of most similar *rrn* genes (*rrnA*, *-B*, *-C*, *-D*, *-E*) contains those located nearest the replication origin of the *Salmonella* chromosome (see Figure 2). All of the loci in this cluster have an intervening sequence in helix 25 of their 23S RNA gene that is removed from the messenger RNA prior to ribosome assembly (Mattatall and Sanderson 1996, 1998). The most dissimilar loci (*rrnH* and *rrnG*) show ~1.5% sequence difference. The *rrnG* locus has an intervening sequence only in helix 45 of its 23S RNA gene. The *rrnH* gene has an intervening sequence in both helix 25 and helix 45.

